Comparison of Semi-Physical and Black-Box Bushing Model for Vehicle Dynamics Simulation

Jeong-Hyun Sohn, Seung-Kyu Lee
School of Mechanical Engineering, Pukyong National University,
San 100, Yongdang-dong, Nam-gu, Busan 608-739, Korea
Jin-Kyu Ok, Wan-Suk Yoo*
School of Mechanical Engineering, Pusan National University,
San 30, Jangjeon-dong, Geumjung-gu, Busan 609-735, Korea

Since bushing components have highly nonlinear characteristics according to the amplitude and the frequency, it is hard to derive a mathematical modeling of the bushing. In this paper, a semi-physical bushing model and a black-box bushing model are derived and compared. A Bouc-Wen hysteretic model is employed to derive a semi-physical model and an artificial neural network algorithm is used to make a black-box bushing model. A 3-axes MTS rubber test machine is used to capture the bushing characteristics. Sine excitation tests based on the different frequencies and different amplitudes are performed to find out the bushing characteristics. Random test results are also used to generate the coefficients of a semi-physical model and weighting factors of the black-box model. Random simulations are carried out to verify the bushing models and the results are compared with each other according to the numerical efficiency and accuracy.

Key Words : Bushing, Semi-Physical Model, Black-Box Model, Artificial Neural Network

1. Introduction

The multi-body dynamic analysis techniques using high-performance computers have been effective tools for the analysis and design in the machine and automobile industries. Many researchers have conducted several studies to improve the accuracy and the computational efficiency of these computer-aided analysis techniques. In the automobile industry, computer-aided simulations have been widely used for motion and load analyses of a ground vehicle under various conditions such as bumps and steering inputs. Particularly, in vehicle suspension systems, bushing elements are usually used to improve the ride quality and the components durability. The bushing element is a hollow cylinder connecting the outer steel cylindrical sleeve and the inner steel cylindrical rod. The inner rod is connected to the chassis and is used to transfer forces from the wheel to the chassis. Due to the rubber materials in the bushing, it has nonlinear characteristics for both load amplitudes and frequencies, and also hysteretic responses for the repeated vibration excitations. Since the characteristics of the rubber bushing affects significantly to the accuracy of the vehicle dynamic simulation result, it should be accurately considered in the vehicle suspension model. The bushing forces depend not only on the instantaneous deformation but also on the past history of deformation. As a result, the hysteretic restoring force cannot be expressed by an algebraic function of the instantaneous displacement and velocity. This history-dependent characteris-

* Corresponding Author,
E-mail : wsyoo@pusan.ac.kr
TEL : +82-51-510-2328; **FAX** : +82-51-581-8514
School of Mechanical Engineering, Pusan National University, San 30, Jangjeon-dong, Geumjung-gu, Busan 609-735, Korea. (Manuscript **Received** August 10, 2006; **Revised** December 8, 2006)

tic of a bushing renders the hysteretic systems more difficult to model and analyze than other non-linear systems.

The multi-body dynamic analysis programs such as ADAMS and RecurDyn generally adopt the Kelvin-Voight model for the bushing element. This model treats the bushing element as a linear combination of three translational spring-dampers and three rotational spring-dampers. However, this type of bushing model cannot properly generate the hysteretic behavior of the bushing element.

High-accuracy models of the bushing can be classified as two different model classes : semi-physical model and black-box model. As the semi-physical models, there are Bingham visco-plastic model and a modified Bouc-Wen model (Spencer model). Also in the class of black-box models, there are multi-variable polynomials, multi-layer feedforward neural network (NN), radial-basis neural networks (RBF), multi-variable splines, wavelets, etc.

As a semi-physical model, Bouc-Wen (1975) model has been widely used to represent non-linear hysteretic systems. The Bouc-Wen differential model is originally proposed by Bouc and subsequently generalized by other researchers. This nonlinear differential equation model includes the time history-dependent nature of the hysteretic force. For a given time history of the displacement, the restoring force is completely specified by the differential model, without need of empirical rules or additional conductions. This model reflects local history dependence through introducing an extra state variable. Through appropriate choice of parameters in the model, it can represent a wide variety of softening or hardening, smoothly varying or nearly bilinear hysteretic behavior. Sain (1998) carried out an initial study of qualitative characteristics. Spencer (1996) developed the phenomenological model of a magneto-rheological damper.

As a black-box model, the artificial neural network algorithm was introduced in modeling the vehicle suspension systems. Barber (2000) suggested the possibility of the artificial neural network for modeling the bushing. Sohn et al (2005) carried out vehicle dynamic simulations using the neural network bushing model.

In this paper, a semi-physical model (Bouc-Wen model) and a black-box model (artificial neural network model) are employed and compared with each other according to the numerical accuracy and numerical efficiency. A 3-axes MTS rubber tester was used to capture the practical dynamic behavior of the bushing. The experimental procedure and test result of the bushing element are described in chapter 2. The Bouc-Wen bushing model is introduced in the chapter 3 and the artificial neural network model is explained in the chapter 4. The results are shown and compared in the chapter 5 and conclusions are shown in the chapter 6.

2. Experiments

All the bushing tests were conducted by 3-axes MTS testing machine as shown in Fig. 1, and the

Table 1 Specifications of bushing tester

Model name	3-axis Elastomer Testing System
Max. Dyn. force	25.0 [kN]
Max. Static force	37.5 [kN]
Max. Dyn. length	25.0 [mm]
Frequency	0.1-80.0 [Hz]
Data acquisition rate	over 6.0 [kHz]

Fig. 1 Test machine

specifications of the machine are shown in Table 1. The configuration and specifications of the bushing used in experiment is shown in Fig. 2 and in Table 2, respectively.

The harmonic tests were conducted by using sinusoidal vibration wave form. The tests were carried out with four different frequencies as shown in Kuo (1997), that is, 1, 10, 20, and 30 Hz. The corresponding amplitudes were, 0.5, 1.0, 2.0, and 3.0 mm, respectively. Since the power spectral density of the bushing load measured from the proving ground test durability analysis typically exhibits a peak value in the range of 10-15 Hz, the maximum frequency for the test was conservatively set at 20 Hz. The forces on the rubber bush due to change of the amplitude and the frequency were measured for duration of 10 seconds. Figure 3 shows the radial bushing force due to the sine wave excitation at 10 Hz. The more amplitude increases, the higher bushing force becomes. Figure 4 shows the radial bushing force due to the sine wave excitation with the amplitude of 3 mm. The more frequency increases, the softer bushing stiffness becomes.

Table 2 Specifications of bushing (mm)

Outer steel diameter (do)	50
Inner steel diameter (di)	15
Length (l)	63
Outer steel thickness (t)	3

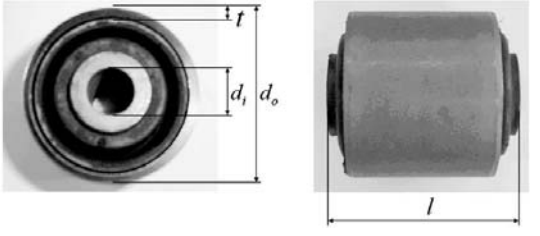

Fig. 2 Bushing configurations

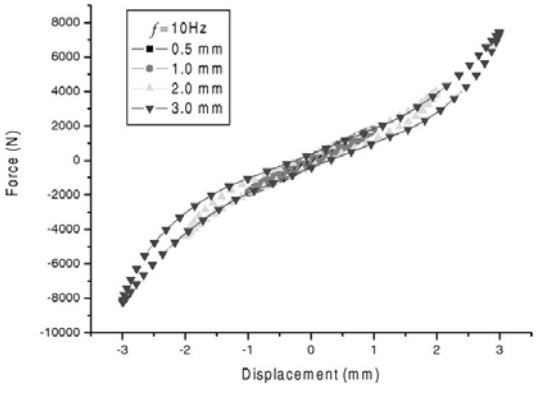

Fig. 3 Radial bushing force (10 Hz sine wave)

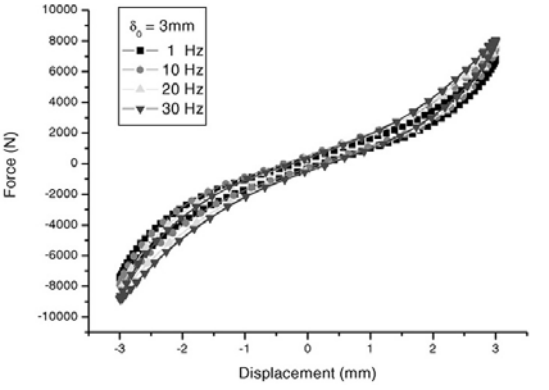

Fig. 4 Radial bushing force (3 mm amplitude sine wave)

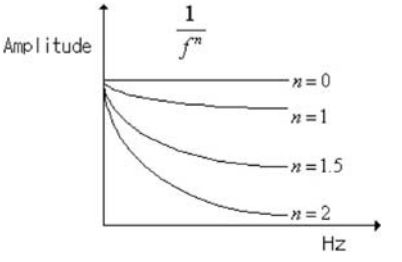

Fig. 5 Amplitude of the random input

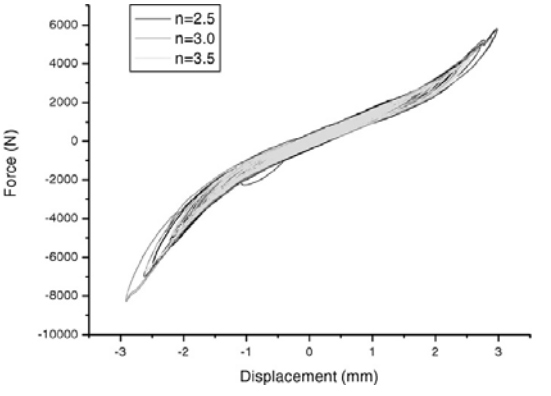

Fig. 6 Bushing force depending on random input

The random tests were carried out to make the Bouc-Wen and neural network bushing model. The random input signal was generated by using CRPC III of the MTS machine. According to the 'n' value, the amplitude is changed as shown in Fig. 5. In this study, the peak value of the amplitude is set to 2 mm.

3. Semi-Physical Model

Figure 7 represents the Bouc-Wen hysteretic bushing model used in this study. In this model, the restoring force and deformation are connected through a nonlinear differential equation containing unspecified loop parameters. By choosing the loop parameters properly, it is possible to generate a large variety of different shapes of hysteretic loops. By using the Bouc-Wen model, the restoring force-displacement relation of a hysteretic bushing can be expressed in terms of the following non-linear differential equations as shown in Spencer (1996) and Wong (1994).

$$\dot{z}_1=(\dot{x}-\dot{y})\left[A_1-\{\gamma_1+\beta_1\,\mathrm{sgn}(\dot{x}-\dot{y})\,\mathrm{sgn}(z_1)\}|z_1|^{n_1}\right] \quad (1)$$

$$\dot{z}_2=(\dot{x}-\dot{w})\left[A_2-\{\gamma_2+\beta_2\,\mathrm{sgn}(\dot{x}-\dot{w})\,\mathrm{sgn}(z_2)\}|z_2|^{n_2}\right] \quad (2)$$

$$\dot{y}=\frac{1}{c_1}\{c_1\dot{x}+k_1(x-y)-k_0y+\alpha_1z_1\} \quad (3)$$

$$\dot{w}=\frac{1}{c_0+c_2}\{c_2\dot{x}+k_2(x-w)+\alpha_2z_2\} \quad (4)$$

$$F=k_0y+c_0\dot{w} \quad (5)$$

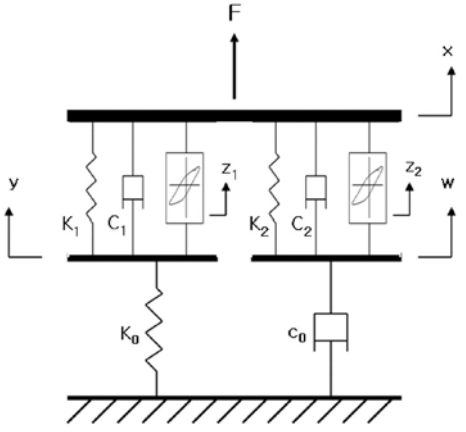

Fig. 7 Proposed Bouc-Wen bushing model

where $x(t)$ represent the displacements. Two hysteretic auxiliary variables $z_1(t)$ and $z_2(t)$ are employed to represent the hysteretic behavior. The dot over a variable denotes the differentiation of the variable with respect to time. Other parameters are determined from the identification procedures.

Identification procedures:

Bouc-Wen differential model of a hysteretic curve can be used to curve-fit any hysteretic traces with suitable choice of the model parameters. The parameters of differential hysteretic loop are estimated from the system identification, which involves estimation of unspecified parameters of an assumed or known model. Sixteen undetermined parameters need to be identified from the experimental data in order to complete this model.

When the system is governed by differential or difference equations, or when the model is intended to predict future response of a system, a time-domain model will eventually be required. Thus only time-domain parametric identification methods are considered in this paper.

A root mean square (rms) error function can be defined as;

$$E=\sqrt{\frac{1}{m}\sum_{i=1}^{m}[F_{\exp}-F_{pre}]^2} \quad (6)$$

subject to

$$A_1, A_2\geq 1,\ \beta_1, \beta_2\geq 0,\ \beta_1+\gamma_1>0,\ \beta_2-\gamma_2>0$$

Where $F_{\exp}$ is the bushing force obtained from experiments and F_{pre} is time points and is the output force from the simulations. And $A_1, A_2, \beta_1, \beta_2, \gamma_1, \gamma_2$ are the parameters in Eqs. (1) ~ (4), respectively.

By minimizing the error function E globally, optimal values of these 16 parameters can thus be determined. The constraint equations in Eq. (6) can be found in Sain (1998).

The VisualDOC program was employed to find the optimal parameters. VisualDOC is a general-purpose optimization tool that allows the user to quickly apply design optimization capabilities to any types of problems. VisualDOC can perform

Table 3 Optimum parameters from the identification

Parameter	Optimum value	Parameter	Optimum value
c_0	299.401	c_2	1.825
k_0	2186.63	k_2	0.526
β_1	1.875	β_2	5.023
γ_1	−10.991	γ_2	−1.758
n_1	0.7795	n_2	0.969
α_1	0.6125	α_2	5.983
c_1	0.805	A_1	2436.323
k_1	1453.895	A_2	79.536

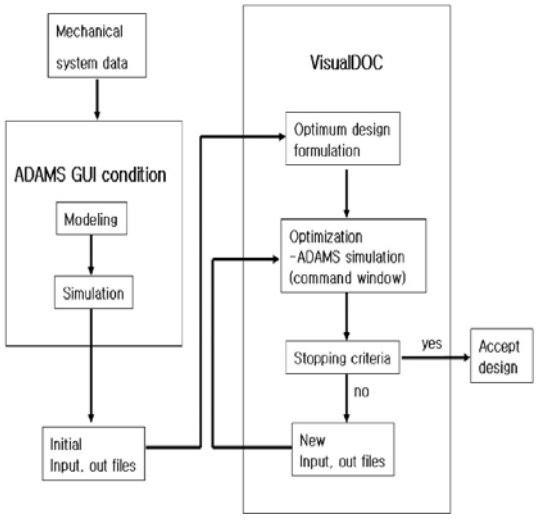

Fig. 8 Identification procedure chart

linear, non-linear, constrained and unconstrained as well as integer, discrete and mixed optimization. Gradient-based, non-gradient based, and response surface approximate optimization algorithms are also available. In this study, the genetic algorithms (GA) is adopted to solve this identification problem as shown in Ok (2006). Fig. 8 shows how to link ADAMS and VisualDOC. Parameters obtained from the identification procedure are shown in Table 3.

4. Black-Box Model

Since the rubber bush has hysteretic characteristics, the inputs and outputs of the previous steps

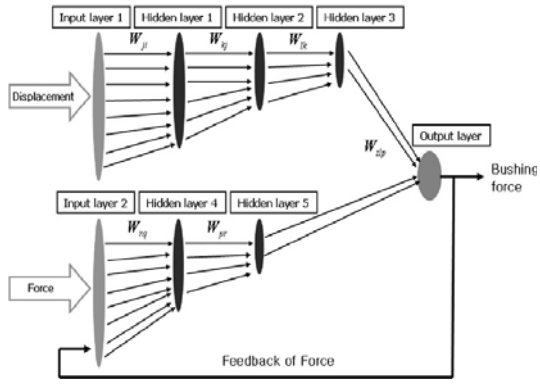

Fig. 9 Structure of the neural network used in this study

affect the current outputs. Therefore, inputs and outputs of the past are used as the input data of the current step. The input components of the neural network are selected from the current displacement, the past displacement and the past outputs. The value of the output layer is the rubber bush force. Through several trial-and-error processes, the structure of the model and the number of neuron of hidden layers were set as shown in Fig. 9. The relation between the input and the output is represented by the following equation ;

$$y_k = f(u_k,\ u_{k-1},\ \cdots,\ u_{k-m},\ y_{k-1},\ \cdots,\ y_{k-N}) \quad (7)$$

where y_k represents the output of k-th pattern, u_k is the input of k-th pattern, m indicates the number of previous input data, and N means the number of pre-step output.

In this study, the rubber bush characteristics were measured by using the MTS machine. The force data corresponding to the displacement of the rubber bush were obtained by using RPCIII software installed in the machine. Deformations and forces were divided by the maximum value of those, respectively. Then, the values are processed by the hyperbolic tangent sigmoid function. SIMULINK was used to interface with MATLAB and ADAMS. Under the SIMULINK environment, ADAMS produces bushing deformation data and these data are transferred to MATLAB. Then, MATLAB calculates bushing force data and these data are used for the next step calculation of ADAMS. Fig. 9 shows the neural network structure used in this study and Fig. 10 is

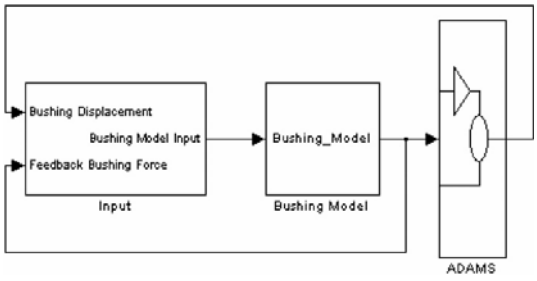

Fig. 10 Structure of the neural network used in this study

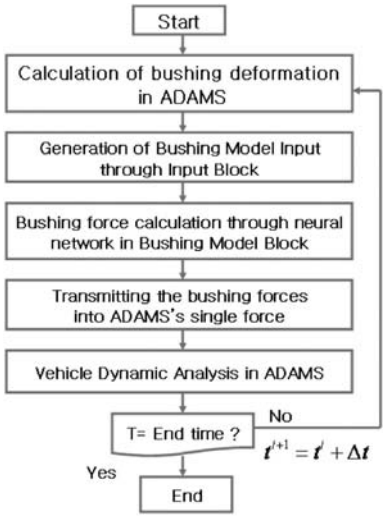

Fig. 11 Flow chart of the bushing force calculation

the SIMULINK structure. Fig. 11 represents the flow chart of bushing force calculation.

5. Comparison of Two Models

Figure 12 shows the excitation input data for the identification of the Bouc-Wen model and artificial neural network model. Fig. 13 represents the bushing forces versus displacement of two models. In the figure, 'Exp' means the experimental result, 'ANN' is the artificial neural network result, and 'BW' represents the Bouc-Wen result. Fig. 14 is the excitation input data for verification of the models. Figs. 15 and 16 represent the bushing forces versus time, and the bushing force versus displacement, respectively. Results of two models show good agreements to the experiments.

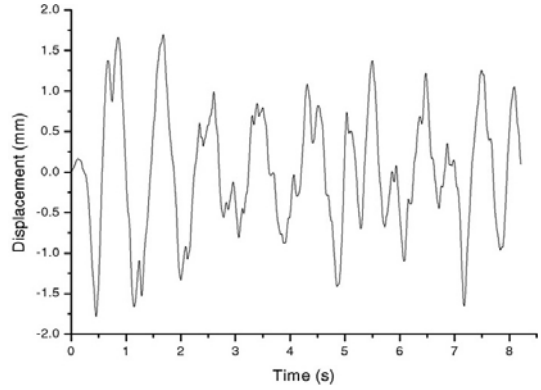

Fig. 12 Random excitation input (for identification)

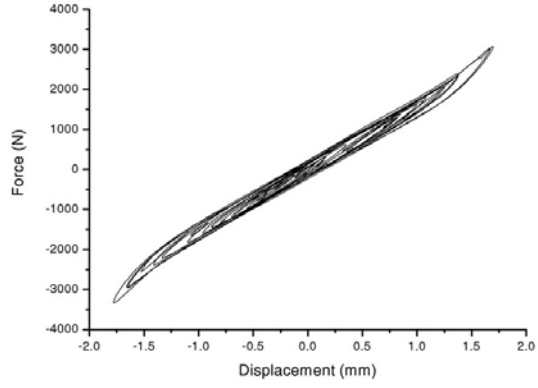

Fig. 13 Forces vs displacement (for identification)

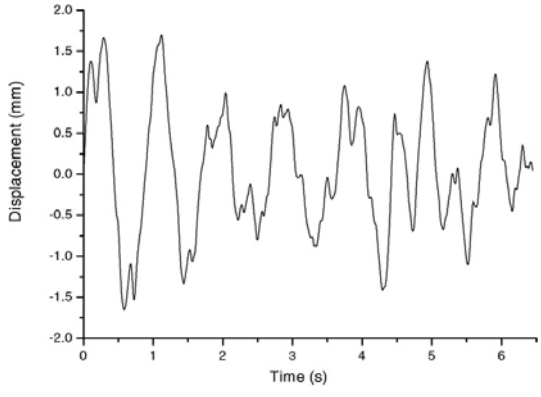

Fig. 14 Random excitation input (for verification)

RMS ratio and ESR are defined as the followings ;

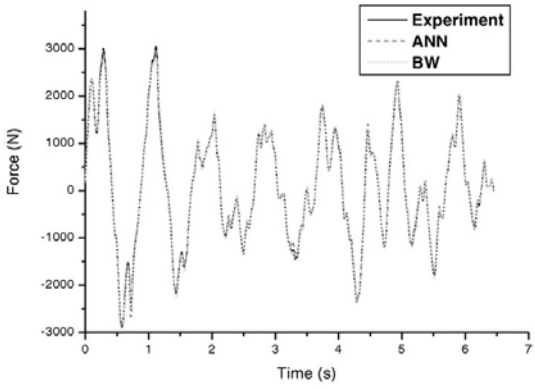

Fig. 15 Comparisons of the forces (for verification)

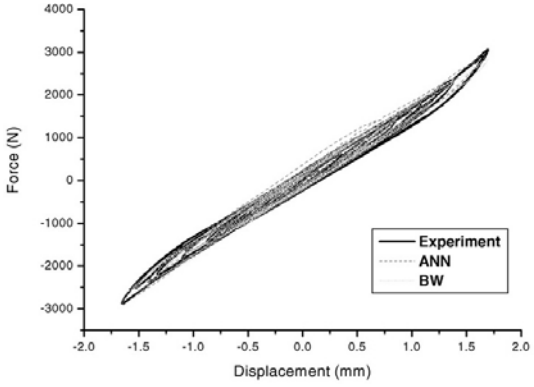

Fig. 16 Forces vs displacement (for verification)

$$\text{RMS ratio}=\frac{\sqrt{\frac{1}{T}\sum_{t=1}^{T}(F_{\exp}(t)-F_{pre}(t))^2}}{\sqrt{\frac{1}{2}\sum_{t=1}^{T}(F_{\exp}(t))^2}} \quad (8)$$

$$\text{ESR}=\frac{\frac{1}{T}\sum_{t=1}^{T}(F_{\exp}(x)-F_{pre}(t))^2}{\frac{1}{T}\sum_{t=1}^{T}\left(F_{\exp}(t)-\left(\frac{1}{T}\sum_{t=1}^{T}F_{\exp}(i)\right)\right)^2} \quad (9)$$

RMS ratio is the ratio between the RMS of the experiment result and the RMS of the simulation error. ESR is the error-to-signal-ratio of the estimated model. As a matter of fact, it is the ratio between the variance of the estimation error and the variance of the output. ESR lies in the range $[0\,;1]$; ESR=1 means that the model only predicts the average value of the output. ESR=0 means that the model exactly predicts the output of the system. Table 4 shows the comparison results of numerical accuracy and Table 5 represents the comparison results of numerical efficiency, respectively. In this study, Pentium IV with 2.0 GB memory was used. The identification data with 8.22 sec and the verification data with 6.44 sec are used.

Table 4 Comparison of numerical accuracy

	ANN	BW
RMS ratio (%)	4.5	3.7
ESR ratio (%)	0.2	0.1
Maximum error (N)	218.8	248.6
Peak error (N)	56	163.2

Table 5 Comparison of numerical efficiency

	ANN	BW
Identification	263 min	725 min
Verification	22 min	4 sec

In the Table 4, the ANN model gives more accurate results than BW model at peak error. As it can be seen in the Table 5, ANN model gives more efficiency than BW in the identification process, but in the verification, BW takes less time than ANN model. This is because, in the identification process, ANN used only MATLAB but BW experiences interface process with VisualDOC and ADAMS. The genetic algorithms (GA) was employed to find out the parameters in the BW model. The stochastic and randomness nature of GA can be able to avoid local optimum solution. Therefore, it shows the good convergence to the globally optimal solution but takes a long time to calculate the optimal value in the identification process. In the verification process, ANN model takes interface process and has many calculation functions such as 288 times multiplications, 31 times summations and activation function calculations. BW model doesn't need to take the interface process with VisualDOC and simply calculate the uncomplicated differential equations in ADAMS. Therefore, it takes a little simulation time in the verification process and can be used the application of the real time simulation.

6. Conclusions

In this study, the rubber bushing characteristics

were tested by using a MTS 3-axes rubber tester. Sine and random excitations are imposed on the bushing in radial direction. Random test results are used to identify the parameters of the Bouc-Wen model and to extract the weighting factors of the artificial neural network model.

Since the Bouc-Wen model is a semi-physical model including the differential equation, this model can be used to design the bushing element. Also, since it is possible to represent the step response, the bushing force calculation under the steady state equilibrium is possible. However, it requires longer time than Kelvin-Voight to estimate the proper parameters.

Artificial neural network model gives an accurate response under the random input. Through enough learning processes, it can represent all the nonlinear bushing characteristics. However, it takes more time than Bouc-Wen model to calculate the bushing forces.

Results of two models under the random excitation show good agreements to the experiments. Through the comparisons of two models, ANN model is recommended for the numerical accuracy and BW model is suggested for the numerical efficiency.

Acknowledgments

This work was supported by the Korea Science and Engineering Foundation (KOSEF) through the National Research Lab. Program funded by the Ministry of Science and Technology (No. M10400000274-05000027410).

References

Barber, A. J., 2000, Accurate Models for Complex Vehicle Components Using Empirical Methods, SAE 2000-01-1625.

Kuo, E. Y., 1997, "Testing and Characterization of Elastomeric Bushing for Large Deflection Behavior," *SAE Technical report*, No. 970099.

Ok, J. K., Baek, W. K. and Sohn, J. H., 2006, "Kinematic Optimum Design of a Torsion-Beam Suspension Using Genetic Algorithms," *KSAE*, Vol. 14, No. 1, pp. 25～30.

Sain, P. M., Sain, M. K., Spencer, Jr. B. F. and Sain, J. D., 1998, "The Bouc Hysteresis Model : An Initial Study of Qualitative Characteristics," *Proceedings of the American Control Conference*, pp. 2559～2563.

Sohn, J. H. and Baek, W. K., 2005, "Vehicle Dynamic Simulation Including an Artificial Neural Network Bushing Model," *Journal of Mechanical Science and Technology*, Vol. 19, No. 1, pp. 255～264.

Spencer Jr. B. F., Dyke, S. J., Sain, M. K. and Carlson, J. D., 1996, "Phenomenological Model of a Magnetorheological Damper," *ASCE Journal of Engineering mechanics*.

Wen, Y. K., 1975, "Approximate Method for Nonlinear Random Vibration," *Journal of the Engineering Mechanics Division, ASCE*, Vol. 101, No. EM4, pp. 389～401.

Wong, C. W., Ni, Y. Q. and Lau, S. L., 1994, "Steady-State Oscillation of Hysteretic Differential Model. I : Response Analysis," *Journal of Engineering Mechanics*, Vol. 120, No. 11, pp. 2271～2298.